

# **LEGIBILITY NOTICE**

A major purpose of the Technical Information Center is to provide the broadest dissemination possible of information contained in DOE's Research and Development Reports to business, industry, the academic community, and federal, state and local governments.

Although portions of this report are not reproducible, it is being made available in microfiche to facilitate the availability of those parts of the document which are legible.

Received by

AUG 04 1988

Los Alamos National Laboratory is operated by the University of California for the United States Department of Energy under contract W-7405-ENG-36.

LA-UR--88-2006

DE88 014430

TITLE: PRODUCTION AND PROPERTIES OF PERRHENATE-DOPED  
ALKALI HALIDE CRYSTALS

AUTHOR(S): O. H. NESTOR AND J. F. FIGUEIRA

SUBMITTED TO: PROCEEDINGS OF THE 1987 BOULDER DAMAGE SYMPOSIUM

### DISCLAIMER

This report was prepared as an account of work sponsored by an agency of the United States Government. Neither the United States Government nor any agency thereof, nor any of their employees, makes any warranty, express or implied, or assumes any legal liability or responsibility for the accuracy, completeness, or usefulness of any information, apparatus, product, or process disclosed, or represents that its use would not infringe privately owned rights. Reference herein to any specific commercial product, process, or service by trade name, trademark, manufacturer, or otherwise does not necessarily constitute or imply its endorsement, recommendation, or favoring by the United States Government or any agency thereof. The views and opinions of authors expressed herein do not necessarily state or reflect those of the United States Government or any agency thereof.

By acceptance of this article, the publisher recognizes that the U S Government retains a nonexclusive, royalty-free license to publish or reproduce the published form of this contribution, or to allow others to do so, for U S Government purposes

The Los Alamos National Laboratory requests that the publisher identify this article as work performed under the auspices of the U S Department of Energy

MAILED

 **Los Alamos** Los Alamos National Laboratory  
Los Alamos, New Mexico 87545

*mt*

---

# Production and Properties of Perrhenate-doped Alkali Halide Crystals

O. H. Nestor

Harshaw/Filtrol Partnership  
Cleveland, Ohio 44139

and

J. F. Figueira

Los Alamos National Laboratory  
Los Alamos, New Mexico 87545

The growth and selected properties of single crystals of KCl doped with  $\text{ReO}_4^-$  is described. The crystals have been used as saturable absorbers to modulate and control  $\text{CO}_2$  laser radiation.  $\text{ReO}_4^-$  ion concentrations in excess of  $10^{17} \text{ cm}^{-3}$  were achieved in KCl with good optical quality. The room temperature absorption of the  $\text{ReO}_4^-$  ion in KCl was centered at  $936.8 \text{ cm}^{-1}$  with  $1.5 \text{ cm}^{-1}$  linewidth and with absorption cross-section determined to be  $(0.46 \pm 0.02) \times 10^{-16} \text{ cm}^2$ . The addition of  $\text{Li}^+$  as a second dopant resulted in a splitting of the  $\text{ReO}_4^-$  resonance into two components at  $957.5 \text{ cm}^{-1}$  and  $900.7 \text{ cm}^{-1}$ .

The characteristically sharp resonance of  $\text{ReO}_4^-$  was not detected in NaCl grown with  $\text{NaReO}_4$  additions to the melt. Only with addition of  $\text{Ca}^{++}$  as a co-dopant was the  $\text{ReO}_4^-$  resonance observed. The absorption, detected as a very weak resonance through a 92 mm path length, was centered at  $946.0 \text{ cm}^{-1}$  with linewidth of  $6 \text{ cm}^{-1}$ , overlapping the P(20) transition in the 10 micron  $\text{CO}_2$  band.

Key words: alkali halides; Bridgman-Stockbarger;  $\text{CO}_2$  laser radiation; crystal growth; dopant distribution; double-doped crystals; non-linear material; perrhenate ion absorption; potassium chloride; saturable absorber; sodium chloride.

## 1. Introduction

In a collaborative program between Los Alamos National Laboratory and Cornell University, investigators identified a new class of nonlinear materials that have a variety of potential applications to  $\text{CO}_2$  lasers [1]. These materials are based on the selective introduction of impurity ions into normally transparent alkali halides. The ions are optically active in the infrared, producing absorptions in the 10 micron wavelength region. The first successful demonstration of this concept was made using a KCl crystal host doped with the perrhenate ion  $\text{ReO}_4^-$ . This material has been successfully used as a room-temperature passive pulse compressor for P(28)-transition  $\text{CO}_2$  laser pulses [2] and as a short pulse generator for P(26) radiation at 105°K using optical free-induction decay [3].

In parallel to the LANL/Cornell program, a collaborative effort between LANL and Harshaw/Filtrol was undertaken to identify potential problems in producing large crystals of perrhenate doped alkali halides. The program was designed to produce large crystals of  $\text{KCl}:\text{ReO}_4^-$  with the eventual extension to NaCl single crystal and hot forged hosts. Of particular interest were the dopant concentrations achievable and the associated optical quality, particularly since residual strains in the Czochralski(Cz)-grown Cornell crystals completely destroyed their infrared optical quality. The approach at Harshaw was based on another melt-growth process, the Bridgman-Stockbarger (B-S) technique, successfully applied in the production of large NaCl windows for the Antares project at Los Alamos.

An additional point of interest in the present work was the possibility that the perrhenate absorption in NaCl would be shifted to the region of the P(20)  $\text{CO}_2$  transition at  $944.2 \text{ cm}^{-1}$  and hence that saturable absorption might be realized for this dominant  $\text{CO}_2$  laser line. This possibility was projected by the LANL/Cornell team upon considering the size of the perrhenate ion relative to the lattice parameters of KCl (3.2Å) and NaCl (2.8Å).

The perrhenate ion is estimated to measure approximately 3.1 Å in radius, based on similarities between the perrhenates and periodates of potassium as well as of sodium [4], and the

published I-O bond distance in the periodate ( $\text{IO}_4^-$ ) ion[5]. The perrhenate ion is then tightly constrained by the crystal field of either host lattice, KCl or NaCl, but more so in NaCl wherein the restoring force for the vibrational mode is effectively greater and the resonance frequency is accordingly higher.

Because of the dopant-lattice size relationship, it can be expected that the segregation coefficient, ratio of dopant level in the solid phase to that in the melt, would be  $\ll 1$  for both the B-S and Cz melt processes and that there would be a large variation in dopant concentration along the length of the crystal.

## 2. Crystal Production and Evaluation

The crystals produced in this investigation were grown by the Bridgman-Stockbarger process. Growth materials were melted and crystallized in platinum crucibles in selected gases at one atmosphere pressure. A series of KCl crystals was grown in helium and several crystals were grown in argon. NaCl crystals were grown in  $\text{N}_2$ , air or  $\text{O}_2$ , options spanning a range of possible effects on the oxidation state of the dopant.

Starting materials for growth of doped KCl crystals were once-grown crystals produced from Harshaw-purified KCl powder plus  $\text{KReO}_4$  powder (4N purity from Cerac, Inc.) covering decade steps in the range 0.001-10. weight percent (0.00026 - 2.5 mol percent). Starting materials for doped NaCl crystals were Harshaw-purified NaCl powder plus  $\text{NaReO}_4$  powder (4N purity from Apache Chemicals, Inc.) added at levels of 0.005, 0.10, 1.0 and 10.0 weight percent (0.0011-2.1 mol percent) in a series of runs. Anticipating a segregation coefficient  $\ll 1$  and rather limited melt stirring during growth, the dopant was concentrated in the lower (first-to-be-solidified) end of the crucible with the intent of reducing the variation in  $\text{ReO}_4^-$  content along the length of the crystal.

Double-doped crystals of KCl and NaCl were grown with the second dopant selected to adjust the crystal lattice for a desired effect on the  $\text{ReO}_4^-$  absorption peak. The second dopant for KCl was lithium, added as  $\text{LiCl}$ , and for NaCl it was calcium, added as  $\text{CaCl}_2$ .

Crystals were grown at rates of 1.25-1.60 mm/hr to sizes ranging from 36 mm diameter x 82 mm length to 64 mm diameter x 195 mm length. Samples were taken for transmission spectroscopy, dopant analysis and optical evaluation. The primary spectroscopic evaluations were done with a Nicole Fast Fourier Transform Spectrometer. Perrhenate concentrations were established by neutron activation analysis and by a standard colorimetric technique, assuming all rhenium present as  $\text{ReO}_4^-$ . Samples were examined for Tyndall scattering and, under polarized white light, for strain.

## 3. Results

### 3.1 KCl

#### 3.1.1 Crystal Quality

Figure 1 shows a 64 mm diameter x 190 mm long crystal grown from a charge containing 0.26 mol percent (1.0 weight percent)  $\text{KReO}_4$  at loading and sections of the KCl crystal double-doped with  $\text{ReO}_4^-$  and  $\text{Li}^+$ . The KCl: $\text{ReO}_4^-$  crystals grown in this work were generally of good internal quality except at high dopant levels. Strain as viewed between cross polarizers was at a very low level, an improvement sought relative to the original Czochralski-grown crystals (Figure 2). Typical bulk defects encountered with dopant additions at or below 0.26 mol percent  $\text{KReO}_4$  were low-to-moderate haze and small discrete scattering centers, such as gas bubbles or voids or perhaps particulate inclusions.

Surface defects were encountered in some of the more highly doped crystals. These occurred in the form of pits or channels, such as that evident in the lower crystal in Figure 1, a crystal grown from a melt doped to the 0.26 mol percent level. It is surmised that there occurs a nucleation process for such defects that depends on the local melt composition and the proximity of a surface, such as the crucible wall. This is suggested further by inclusions at the crystal wall (Figure 3) found in one of the crystals doped with 0.26 mol percent  $\text{KReO}_4$ . A possible extension of such process was found in the interior of a crystal grown from a melt of 2.5 mol percent  $\text{KReO}_4$ ; therein a 39 mm long channel was nucleated in the surrounds of optically clear crystal and grew to a diameter in excess of 1 mm. A scanning electron microgram of this defect is shown in Figure 4. It was shown to contain Re, K and Cl, the latter in non-stoichiometric

ratio. This crystal gave indication of an upper limit on the  $\text{KReO}_4$  concentration in the form of high density of inclusions and boundaries between  $5^\circ$ - $10^\circ$  misoriented grains, both evident in the latter-grown part of the crystal (Figure 5).

### 3.1.2 $\text{ReO}_4^-$ Distribution

The dopant distributions measured in this work require that the surface and bulk concentrations be distinguished. This was suggested by the findings discussed above and further by analytical results shown in Figure 6 applying to a slab taken from the cone section of the crystal of Figure 3. The data of Figure 6 represent colorimetric determinations accurate and precise to within 2 percent down to the ppm range. It is seen that an order-of-magnitude difference in the surface to bulk concentrations was measured in this example.

With the segregation coefficient  $\ll 1$  and perfect mixing, a significant increase in dopant content can be expected along the length of the crystal. In order to smooth out the expected variation, the dopant load was concentrated in the cone end of the crucible. Figure 7 shows the variation measured colorimetrically along the surface of two crystals, one grown with a starting concentration of 0.26 mol percent (1.0 wt percent)  $\text{KReO}_4$  in the melt and the other with 0.026 mol percent. The upper curve data point at 1 cm from the start of growth represents the average of the determinations detailed in Figure 6. Order-of-magnitude variation in dopant concentration is seen in the results of Figure 7, even as moderated by the non-uniform initial doping of the charge. The effect of the initial concentration of the dopant is evident. The ensuing decline in dopant concentration is understood to follow from the mixing that occurred (over 40 hours) in the melt. The increase that then follows is that representative of a segregation coefficient  $< 1$ .

The general level of the dopant surface contents of the two crystals surveyed in Figure 7 are not in the same ratio as that of the respective starting compositions: the surface concentrations in general are disproportionately high for the 1.0 wt percent  $\text{KReO}_4$  doping relative to the 0.1 wt percent doping. Again, it is presumed this signals that the wall effect becomes more significant with increasing doping.

Bulk concentration data are shown in Figure 8 as a function of starting compositions. These results are based on neutron activation methodology and apply to slabs normal to the growth direction, taken from 195 mm long crystals at fixed locations corresponding to 90 percent of the crystal grown, a standardizing procedure adopted in light of the longitudinal variation in the  $\text{ReO}_4^-$  concentration. This result indicates that a controllable dopant concentration can be achieved in the bulk material in KCl, with  $\text{ReO}_4^-$  concentrations approaching  $10^{17} \text{ cm}^{-3}$  in highly doped samples.

### 3.1.3 $\text{KCl}(\text{ReO}_4^-)$ Spectroscopy

Figure 9 shows a typical room temperature absorption spectrum of  $\text{KCl}:\text{ReO}_4^-$  in the 10 micron region. Coupling this with neutron activation-determined dopant concentrations yields a value of  $(0.46 \pm 0.02) \times 10^{-16} \text{ cm}^2$  for the absorption cross section at  $936.8 \text{ cm}^{-1}$ . Thus, absorption coefficients in excess of  $4 \text{ cm}^{-1}$  can be obtained in highly doped single crystal samples.

The KCl crystal double-doped with  $\text{Li}^+$  and  $\text{ReO}_4^-$  was of good quality, having only low haze in the first half of a 63 mm diameter x 115 mm long crystal and moderate haze with decorated mosaic boundaries in the second half. The 10 micron absorption for this crystal is characterized by two resonances at  $957.5 \text{ cm}^{-1}$  and  $900.7 \text{ cm}^{-1}$ , instead of the single line at  $936.8 \text{ cm}^{-1}$  seen in  $\text{KCl}:\text{ReO}_4^-$ . This change is attributed to the removal of degeneracy in the fundamental vibrational mode of the  $\text{ReO}_4^-$  ion.

### 3.2 NaCl

Crystals grown from melts charged with 0.022 mol percent (0.1 wt percent)  $\text{NaReO}_4$  surpassed their KCl counterparts in quality. That from a 2.1 mol percent  $\text{NaReO}_4$  melt was comparable to its high-doped KCl counterpart, exhibiting reasonable quality over the first-grown half, but hardly translucent over the last-grown half.

NaCl crystals singly-doped with  $\text{ReO}_4^-$  did not exhibit the sharp resonance characteristic of the  $\text{ReO}_4^-$  ion. They exhibited only broad absorption in the 10 micron wavelength region. Such absorption was attributed to a collective lattice mode of vibration that by experimentation was shown to be extremely difficult to saturate.

Only when  $\text{Ca}^{++}$  was added as a co-dopant was the sharp  $\text{ReO}_4^-$  absorption detected. Growth of NaCl doped with  $\text{ReO}_4^-$  and  $\text{Ca}^{++}$  was predicated on utilizing Ca to expand the NaCl lattice such that the  $\text{ReO}_4^-$  ion could be accommodated [6]. A double-doped crystal, grown in nitrogen from a melt charged with 0.21 mol percent  $\text{NaReO}_4$  plus 0.0062 mol percent  $\text{CaCl}_2$ , exhibited the  $\text{ReO}_4^-$  absorption resonance, though very weakly even through a 92 mm path. The resonance at room temperature is shown in Figure 10. It is centered at  $946.0 \text{ cm}^{-1}$  with bandwidth of  $6 \text{ cm}^{-1}$ , overlapping the desired  $944.2 \text{ cm}^{-1}$  P(20) transition in the 10 micron  $\text{CO}_2$  band. The  $\text{ReO}_4^-$  ion concentration was below the detection threshold of the neutron activation technique ( $2 \times 10^{14}/\text{cm}^3$ ). Based on assuming equal transition probabilities in KCl and NaCl, the estimated average  $\text{ReO}_4^-$  concentration in the spectroscopically probed path was  $1.6 \times 10^{14} \text{ cm}^{-3}$ .

Other double-doped crystals were grown with  $\text{ReO}_4^-/\text{Ca}^{++}$  ratios in the 1-10 range and with  $\text{Ca}^{++}$  up to 0.5 mol percent. These had an absorption peak at  $946 \text{ cm}^{-1}$  with absorption coefficient in the 0.3-0.9 percent/cm range. This is probably too low to be of practical interest for  $\text{CO}_2$  lasers.

#### 4. Summary

This research has shown that  $\text{ReO}_4^-$  ion concentrations in the range  $10^{17} \text{ cm}^{-3}$  and higher can be achieved in large KCl crystals of good optical quality grown by the Bridgman-Stockhager process. KCl: $\text{ReO}_4^-$  crystals exhibiting room-temperature absorption at  $936.8 \text{ cm}^{-1}$  suitable for pulse compression and short pulse generation in the 10 micron  $\text{CO}_2$  band can be produced.

The use of  $\text{Li}^+$  as a second dopant with  $\text{ReO}_4^-$  in KCl yielded resonances at  $957.5 \text{ cm}^{-1}$  and  $900.7 \text{ cm}^{-1}$ , apparently removing degeneracy in the fundamental vibrational mode of the  $\text{ReO}_4^-$  ion.

The characteristically sharp resonance of  $\text{ReO}_4^-$  was not detected in NaCl grown with  $\text{NaReO}_4$  additions to the melt. Only with the addition of  $\text{Ca}^{++}$  as a co-dopant was the  $\text{ReO}_4^-$  resonance detected. The room-temperature absorption was shifted relative to that in KCl and was observed at  $946.0 \text{ cm}^{-1}$  with a  $6 \text{ cm}^{-1}$  bandwidth, hence overlapping the  $944.2 \text{ cm}^{-1}$  P(20) transition. However, this was a very weak absorption, presumed to be so because of low  $\text{ReO}_4^-$  ion concentration even in the  $\text{Ca}^{++}$  expanded lattice.

#### 5. Acknowledgement

The authors are grateful to the following contributors to this investigation: Joseph J. Ursic and David A. Hammond, Harshaw/Filtrol, for the growth of crystals; Arthur F. Greene, Harshaw/Filtrol, for colorimetric determinations of the perrhenate ion distributions; Berle Bunker, LANL, for neutron activation analyses for Re-concentrations; and Albert J. Sievers, Cornell University, for advice concerning double dopant combinations.

#### 6. References

- [1] R. K. Ahrenkiel, J. F. Figueira, C. R. Phipps, Jr., D. J. Dunlavy, S. J. Thomas and A. J. Sievers, "A New Saturable Absorber for the  $\text{CO}_2$  Laser Using Doped KCl," Appl. Phys. Letter. **33**, 705 (1978).
- [2] J. F. Figueira, R. K. Ahrenkiel and D. Dunlavy, "Nonlinear Optical Properties of the Perrhenate Ion in KCl," SPIE Vol. 190, LASL Conference on Optics '79, p. 293 (1979).
- [3] R. K. Ahrenkiel, J. F. Figueira and D. Dunlavy, "Generation of Ultrashort  $\text{CO}_2$  Pulses by Free-Induction Decay in KCl: $\text{ReO}_4$ ," SPIE Vol. 190, LASL Conference on Optics '79, p. 332 (1979).
- [4] R. W. G. Wyckoff, "Crystal Structures" (Interscience Publ. Inc., New York), Table VIIIA. 5.
- [5] A. F. Wells, "Structural Inorganic Chemistry" (Clarendon Press, 1975, 4th Ed.), p. 344.
- [6] The authors gratefully acknowledge this suggestion by Professor A. Sievers, Cornell University.

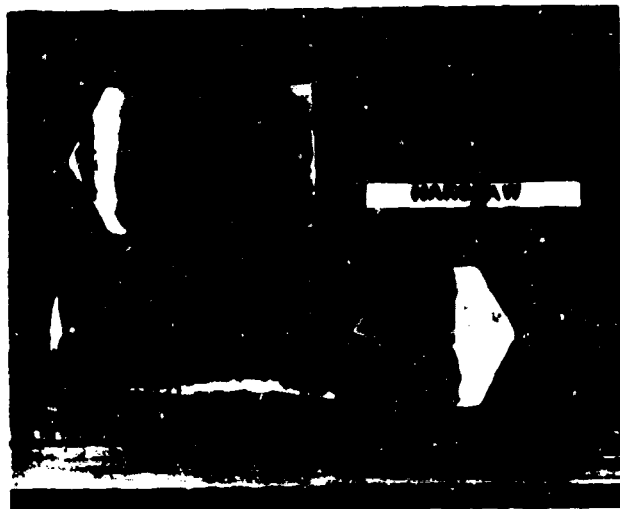


Figure 1. Crystals produced in this program. Lower:  $\text{KCl}(\text{ReO}_4)$  of typical size, 63 mm diameter x 195 mm long. Upper:  $\text{KCl}(\text{ReO}_4, \text{Ca})$ .



Figure 2. Strain comparison of  $\text{KCl}(\text{ReO}_4)$  crystals. Upper: Czochralski-grown in the LANL/Cornell program. Lower: Bridgman-Stockbarger grown in the present program.



Figure 3. Inclusions near periphery of  $\text{KCl}(\text{ReO}_4)$  crystal.

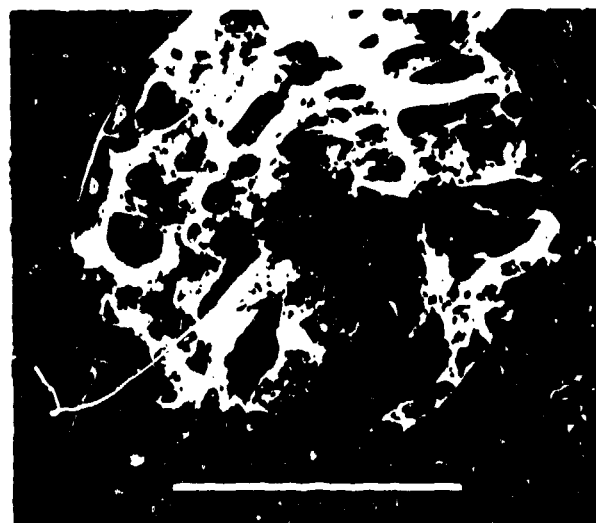


Figure 4. Scanning electron micrograph of defect in a  $\text{KCl}(\text{ReO}_4)$  crystal grown from melt with 2.5 mol %  $\text{KReO}_4$ .



Figure 5. High inclusion density zones and grain boundaries in heavily doped  $\text{KCl}(\text{ReO}_4)$  crystal.

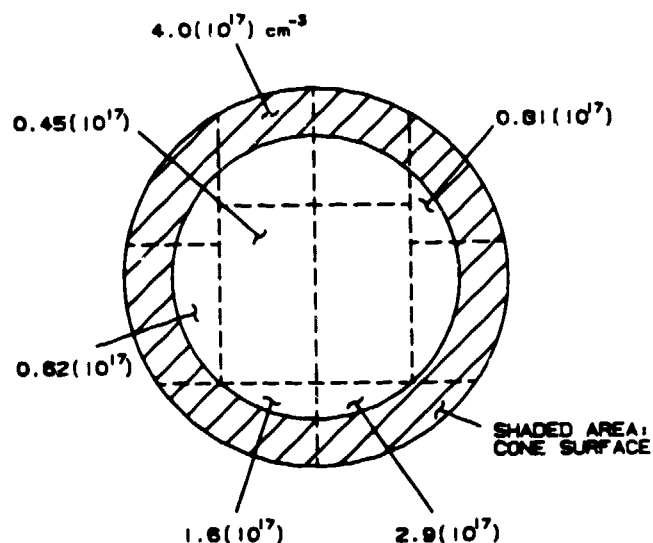


Figure 6. Colorimetrically determined  $\text{ReO}_4^-$  concentration distribution across section of  $\text{KCl}(\text{ReO}_4)$  crystal.

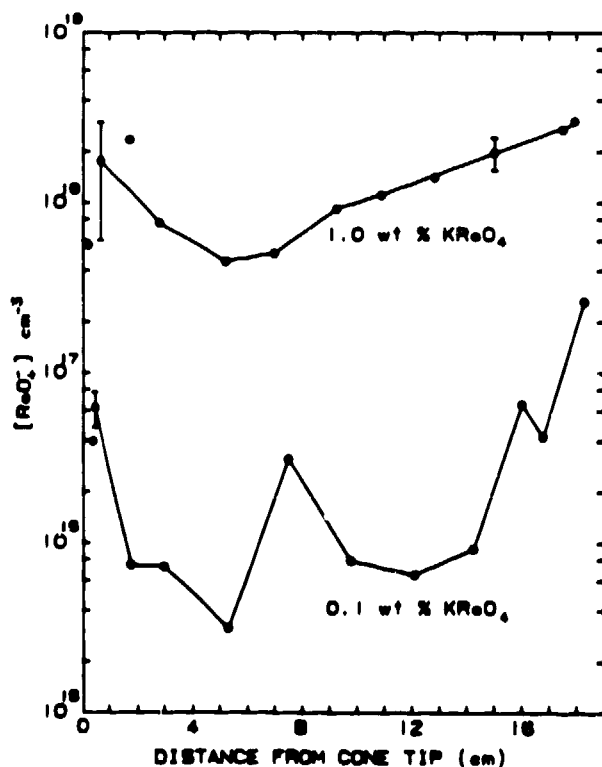


Figure 7. Colorimetrically determined  $\text{ReO}_4^-$  concentration distribution along surface of  $\text{KCl}(\text{ReO}_4)$  crystals.

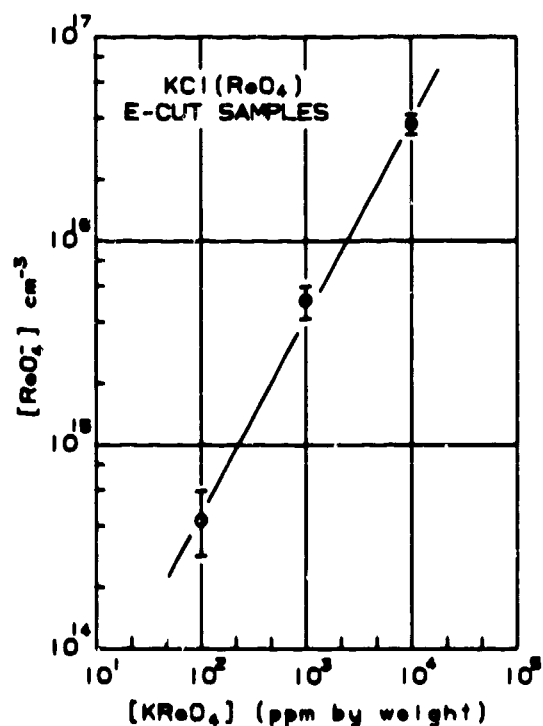


Figure 8. Dopant concentration (determined by neutron activation analysis) within  $\text{KCl}(\text{ReO}_4)$  crystals as a function of the initial dopant loading in the melt.



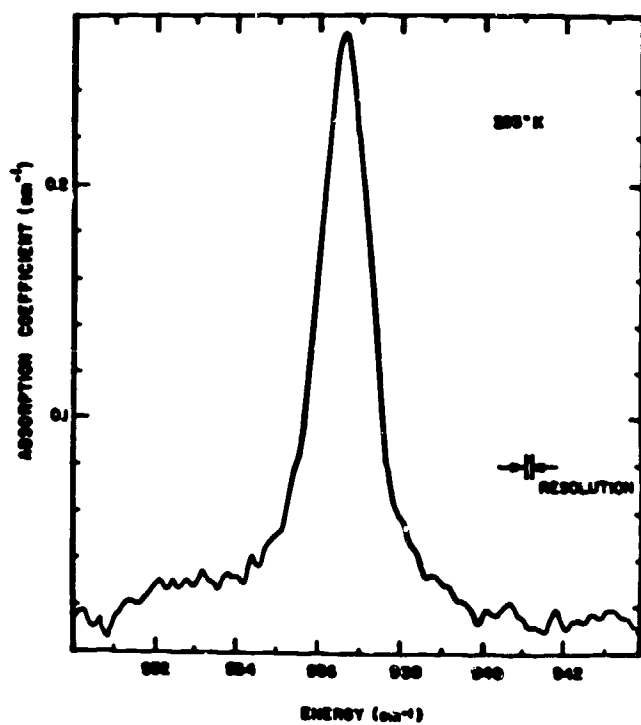


Figure 9. Room temperature absorption spectrum of KCl(ReO<sub>4</sub>) in the 10 micron region.

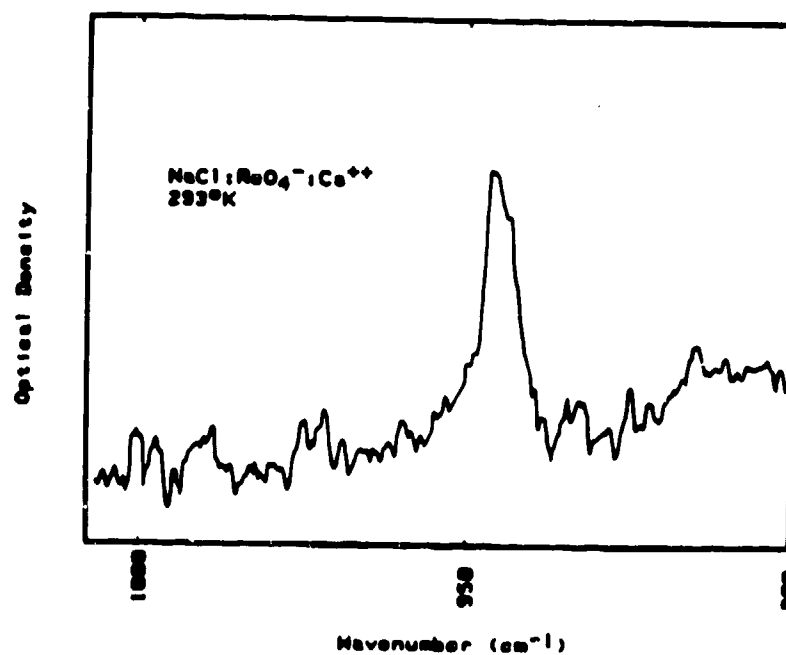


Figure 10. Room temperature absorption spectrum of NaCl(ReO<sub>4</sub>,Ca) in the 10 micron region.

REPRODUCED FROM  
BEST AVAILABLE COPY